

# Entrance-channel potentials in the synthesis of the heaviest nuclei

Vitali Yu. DENISOV<sup>1,2</sup> and Wolfgang Nörenberg<sup>1,3</sup>

<sup>1</sup>Gesellschaft für Schwerionenforschung, Darmstadt, Germany

<sup>2</sup>Institute for Nuclear Research, Kiev, Ukraine

<sup>3</sup>Institut für Kernphysik, Technische Universität Darmstadt, Darmstadt,  
Germany

## Plan

- Capture is the first decisive step for the fusion
- Definition of a semi-microscopic potential (SMP) in the entrance channel
- SMP for cold-fusion systems
- SMP for hot-fusion systems
- SMP for warm-fusion systems
- Conclusion

# Definition of a semi-microscopic potential (SMP) in the entrance channel

The interaction potential  $V(R, \vartheta)$

$$V(R, \vartheta) = E_{12}(R, \vartheta) - E_1 - E_2.$$

In the frozen-density approximation these binding energies are determined by the energy density functional  $\mathcal{E}[\rho_p(\mathbf{r}), \rho_n(\mathbf{r})]$ , i.e.

$$E_{12}(R, \vartheta) = \int \mathcal{E}[\rho_{1p}(\mathbf{r}) + \rho_{2p}(R, \vartheta, \mathbf{r}), \rho_{1n}(\mathbf{r}) + \rho_{2n}(R, \vartheta, \mathbf{r})] d\mathbf{r},$$

$$E_1 = \int \mathcal{E}[\rho_{1p}(\mathbf{r}), \rho_{1n}(\mathbf{r})] d\mathbf{r},$$

$$E_2 = \int \mathcal{E}[\rho_{2p}(\mathbf{r}), \rho_{2n}(\mathbf{r})] d\mathbf{r},$$

where  $\rho_{1p}$ ,  $\rho_{2p}$ ,  $\rho_{1n}$  and  $\rho_{2n}$  are the frozen proton and neutron densities of the spherical nucleus (index 1) and the deformed nucleus (index 2), respectively.

Energy-density functional:

$$\mathcal{E}[\rho_p(\mathbf{r}), \rho_n(\mathbf{r})] = \frac{\hbar^2}{2m}[\tau_p(\mathbf{r}) + \tau_n(\mathbf{r})] + \mathcal{V}_{\text{Skyrme}}(\mathbf{r}) + \mathcal{V}_{\text{Coul}}(\mathbf{r}).$$

$\rho_{1p}(\mathbf{r}), \rho_{2p}(R, \vartheta, \mathbf{r}), \rho_{1n}(\mathbf{r}), \rho_{2n}(R, \vartheta, \mathbf{r}) \Rightarrow$  Hartree-Fock-Bogoliubov (HFB)  
with Skyrme forces.

The kinetic parts for the protons ( $i = p$ ) and neutrons ( $i = n$ )

$$\begin{aligned} \tau_i(\mathbf{r}) = & \frac{3}{5}(3\pi^2)^{2/3} \rho_i^{5/3} + \frac{1}{36} \frac{(\nabla \rho_i)^2}{\rho_i} + \frac{1}{3} \Delta \rho_i \\ & + \frac{1}{6} \frac{\nabla \rho_i \nabla f_i + \rho_i \Delta f_i}{f_i} - \frac{1}{12} \rho_i \left( \frac{\nabla f_i}{f_i} \right)^2 \\ & + \frac{1}{2} \rho_i \left( \frac{2m}{\hbar^2} \frac{W_0}{2} \frac{\nabla(\rho + \rho_i)}{f_i} \right)^2, \end{aligned}$$

where  $W_0$  - the strength of the Skyrme spin-orbit interaction,  $\rho = \rho_p + \rho_n$ ,

$$f_i(\mathbf{r}) = 1 + \frac{2m}{\hbar^2} \left( \frac{3t_1 + 5t_2}{16} + \frac{t_2 x_2}{4} \right) \rho_i(\mathbf{r}).$$

The potential part  $\mathcal{V}_{\text{sk}}$ , Skyrme interaction,

$$\begin{aligned} \mathcal{V}_{\text{Skyrme}}(\mathbf{r}) = & \frac{t_0}{2} \left[ \left(1 + \frac{1}{2} x_0\right) \rho^2 - \left(x_0 + \frac{1}{2}\right) (\rho_p^2 + \rho_n^2) \right] \\ & + \frac{1}{12} t_3 \rho^\alpha \left[ \left(1 + \frac{1}{2} x_3\right) \rho^2 - \left(x_3 + \frac{1}{2}\right) (\rho_p^2 + \rho_n^2) \right] \\ & + \frac{1}{4} \left[ t_1 \left(1 + \frac{1}{2} x_1\right) + t_2 \left(1 + \frac{1}{2} x_2\right) \right] \tau \rho \\ & + \frac{1}{4} \left[ t_2 \left(x_2 + \frac{1}{2}\right) - t_1 \left(x_1 + \frac{1}{2}\right) \right] (\tau_p \rho_p + \tau_n \rho_n) \\ & + \frac{1}{16} \left[ 3t_1 \left(1 + \frac{1}{2} x_1\right) - t_2 \left(1 + \frac{1}{2} x_2\right) \right] (\nabla \rho)^2 \\ & - \frac{1}{16} \left[ 3t_1 \left(x_1 + \frac{1}{2}\right) + t_2 \left(x_2 + \frac{1}{2}\right) \right] \left[ (\nabla \rho_n)^2 + (\nabla \rho_p)^2 \right] \\ & - \frac{W_0^2}{4} \frac{2m}{\hbar^2} \left[ \frac{\rho_p}{f_p} (2\nabla \rho_p + \nabla \rho_n)^2 + \frac{\rho_n}{f_n} (2\nabla \rho_n + \nabla \rho_p)^2 \right], \end{aligned}$$

where  $t_0, t_1, t_2, x_0, x_1, x_2, \alpha$  and  $W_0$  are Skyrme force parameters.

The Coulomb energy density

$$\mathcal{V}_{\text{Coul}}(\mathbf{r}) = \frac{e^2}{2} \rho_p(\mathbf{r}) \int \frac{\rho_p(\mathbf{r}')}{|\mathbf{r} - \mathbf{r}'|} d\mathbf{r}' - \frac{3e^2}{4} \left( \frac{3}{\pi} \right)^{1/3} (\rho_p(\mathbf{r}))^{4/3}.$$

# Entrance channel dynamics

The nuclear interaction time  $\tau_{\text{coll}}$  (collision time)

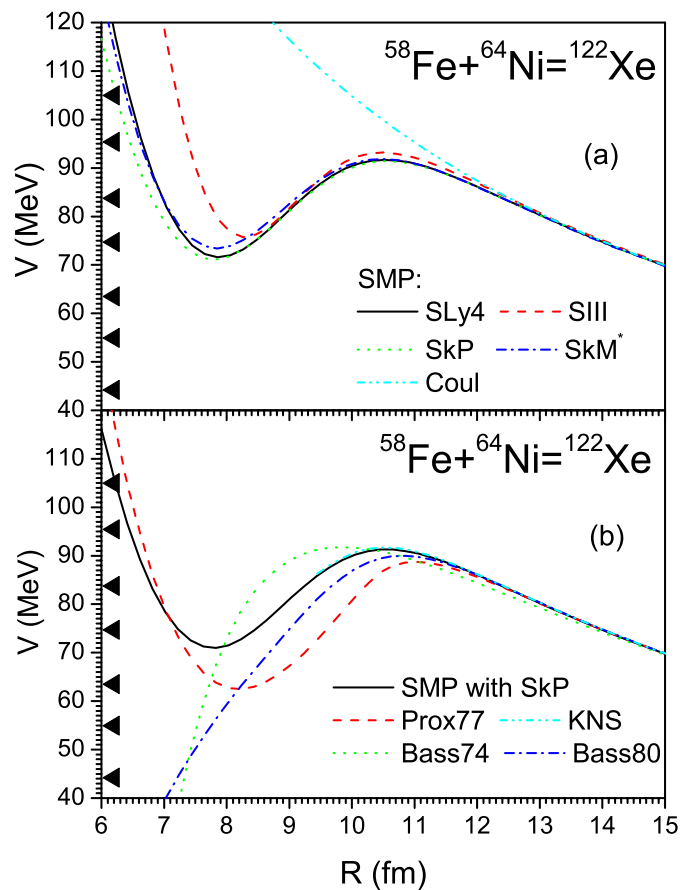
$$\tau_{\text{coll}} \approx \frac{\pi}{\omega_{\text{pocket}}} = \pi \left[ \frac{mA_1A_2}{(A_1 + A_2)V''(R_{\text{pocket}})} \right]^{1/2} \approx 3 \cdot 10^{-22} \text{s}.$$

The relaxation of the intrinsic nuclear state due to nucleon-nucleon interactions  $\tau_{\text{relax}}$  (G.F. Bertsch)

$$\tau_{\text{relax}} \approx \frac{\epsilon_F}{3.2\sigma v_F \rho_0 E^*} \approx \frac{2 \cdot 10^{-22}}{E^*} \text{s} \approx 3 \cdot 10^{-21} \text{s}.$$

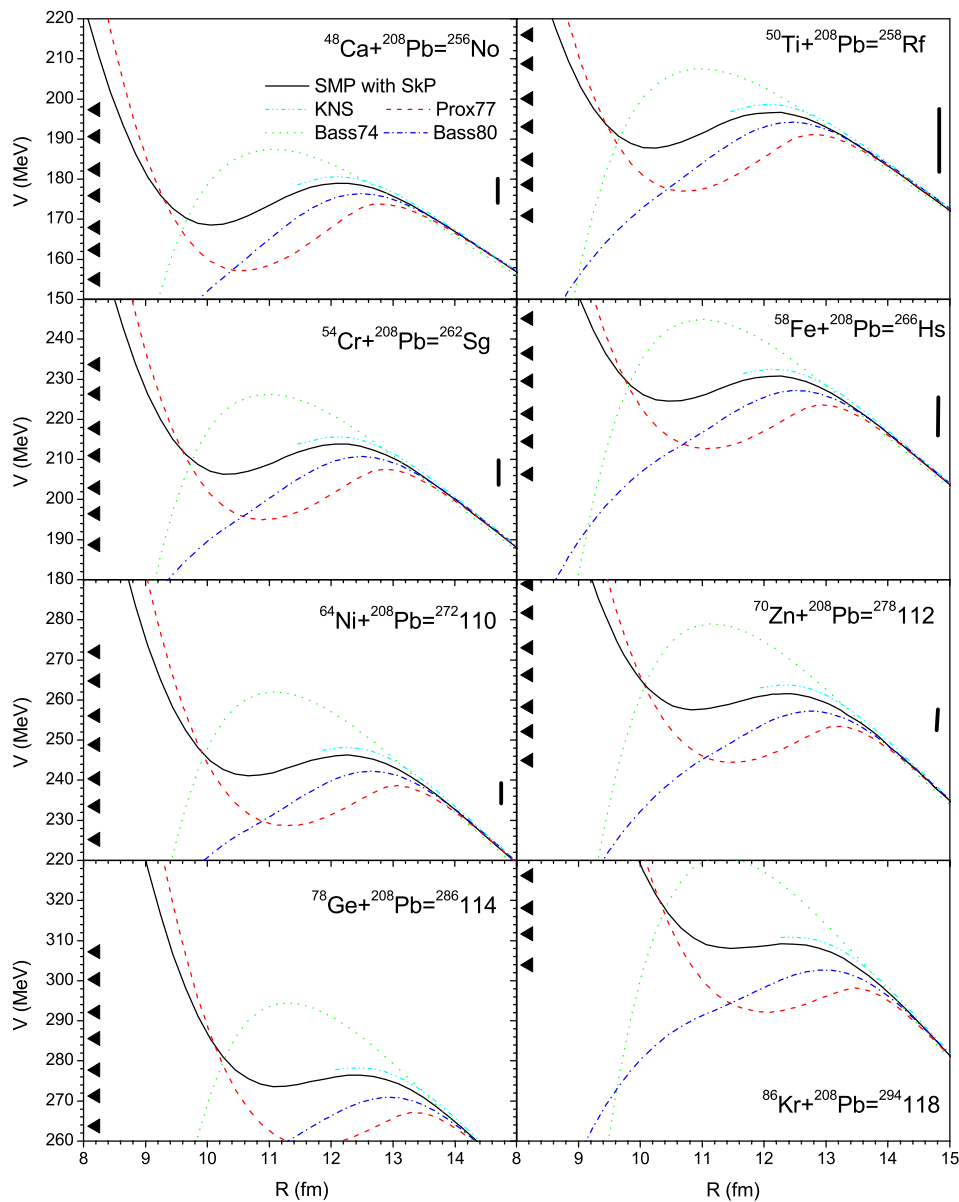
$$\tau_{\text{relax}} \gg \tau_{\text{coll}}.$$

**Conclusion:** Frozen-densities of nucleons in nuclei can be applied for the evaluation of the nucleus-nucleus potential.



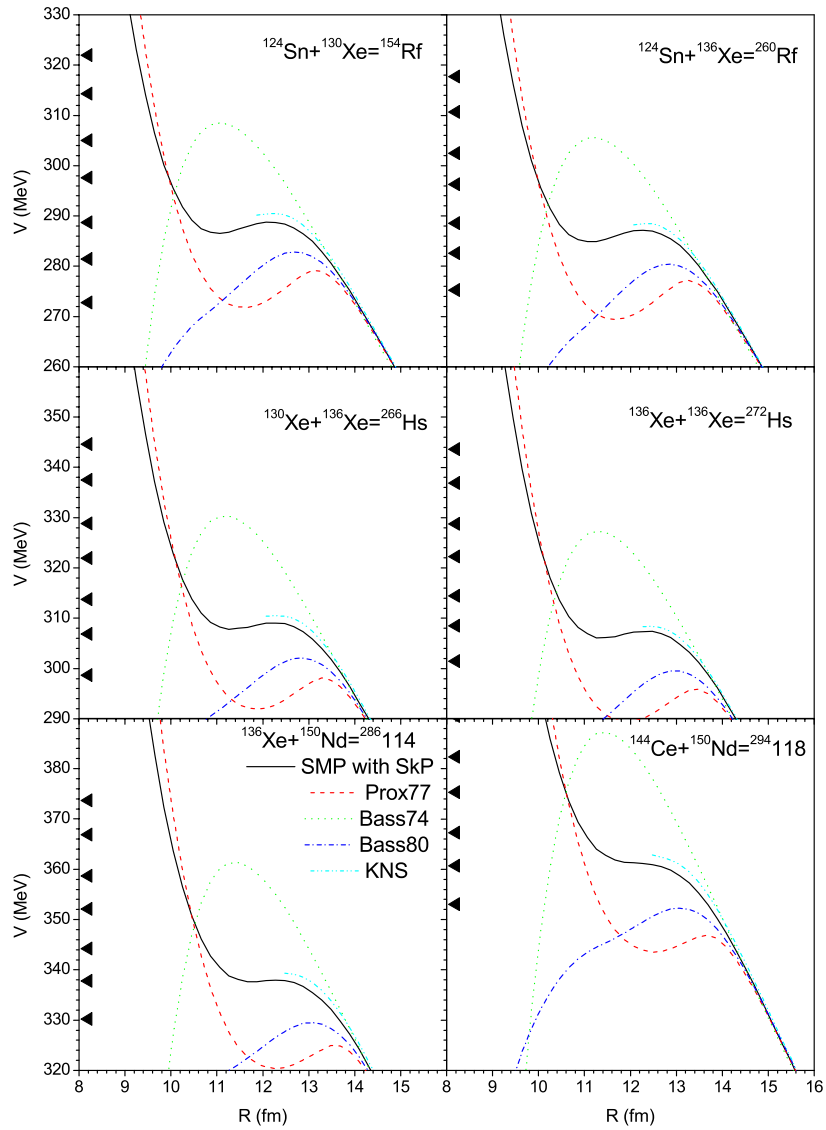
## Main features of SMP in light systems:

- Deep pocket inside the barrier
- Light ions easily fuse after tunneling through or passing over the barrier
- The barrier height and the potential pocket are well above the ground-state energy
- The potential surface exhibits large gradients in the fusion direction driving the system into the compound-nucleus shape
- The barriers obtained with the help Bass-74, Bass-80, Proximity-77 and Krappé-Nix-Sierk (KNS) potentials are spread over a wide interval



- The Bass-74, -80, Prox-77 and KNS interaction potentials are spread over even larger intervals for heavier systems as compared to light system
- The potential pockets are much shallower than for lighter systems and tend to vanish with increasing size of the projectile
- We attribute the observed reduction of the SHE formation with increasing size of the projectile, at least partially, to decreasing pocket depth
- The observed fusion windows lie about 5 to 10 MeV below SMP barriers.
- There is a correlation between the width of fusion window and the depth of potential pocket (cases  $^{50}\text{Ti}+^{208}\text{Pb}$ ,  $^{58}\text{Fe}+^{208}\text{Pb}$  and  $^{64}\text{Ni}+^{208}\text{Pb}$ )

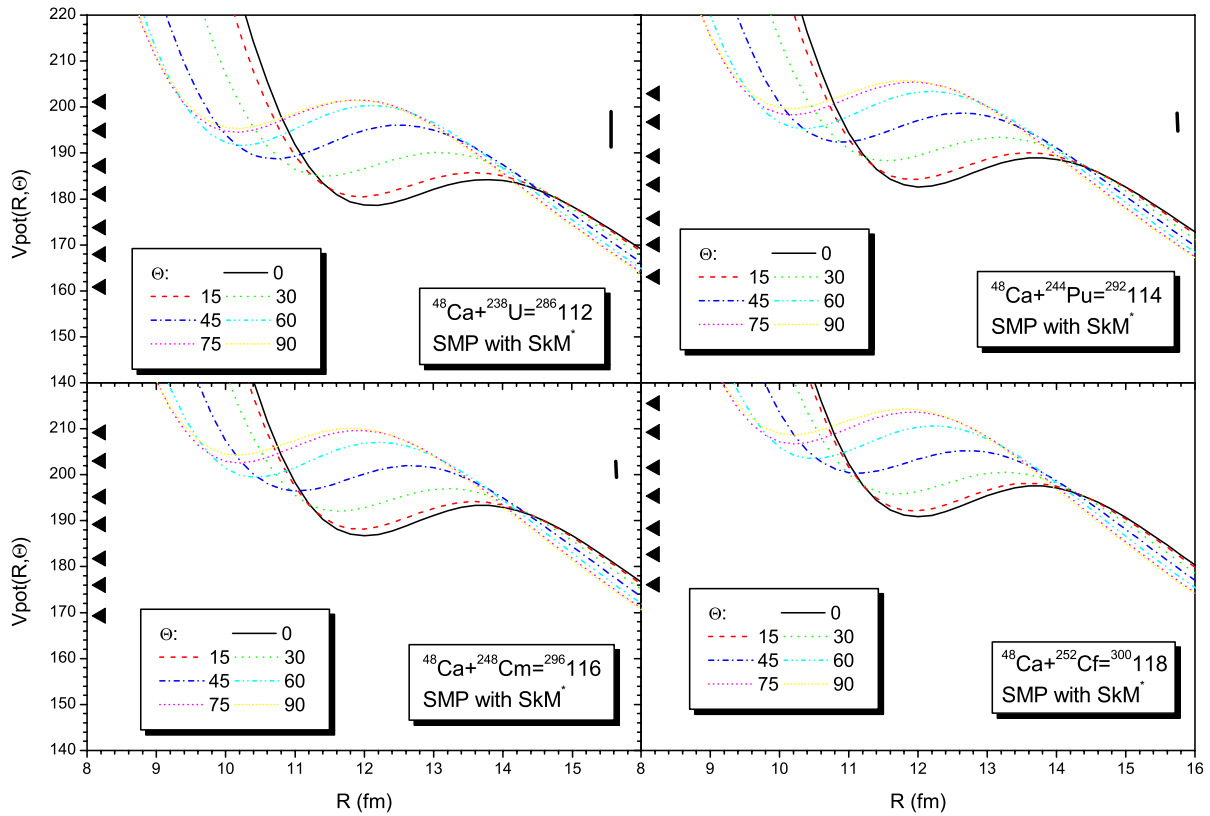
- The difference between the barrier position and the ground-state  $Q$ -value for fusion decreases with increasing charge of the projectile



## Symmetric systems

- The capture process is suppressed by the shallowness of the potential pocket
- The shape of the system at capture is less compact, and hence a longer shape evolution is needed to reach the compound-nucleus shape.  
 ⇒ the formation probability of compound nucleus is reduced due to the larger competition of other decays





Large distances between spherical and prolate nuclei  $\Rightarrow \vartheta = 90^\circ$   
 due to the Coulomb interaction ( $\vartheta = 90^\circ \Leftrightarrow$  side position)

The time for the rotating the deformed nucleus by  $90^\circ$

$$\tau_{\text{rot}} \approx \frac{\pi}{2\omega_{\text{rot}}} = 2 \cdot 10^{-20} \text{ s},$$

where  $\hbar\omega_{\text{rot}} \approx 50 \text{ keV}$ . Typical collision times on the approaching part of the Coulomb trajectory are order  $2 \cdot 10^{-21} \text{ s}$ .

- Strong orientation effect on the barrier and pocket, strongly deformed prolate target
- High excitation energy of compound nucleus
- Fusion relates with side orientation ( $\vartheta \approx 90^\circ$ )
- Fusion suppressed for tip position ( $\vartheta \approx 0^\circ$ )
- The height of the barrier reduces with increasing neutron number

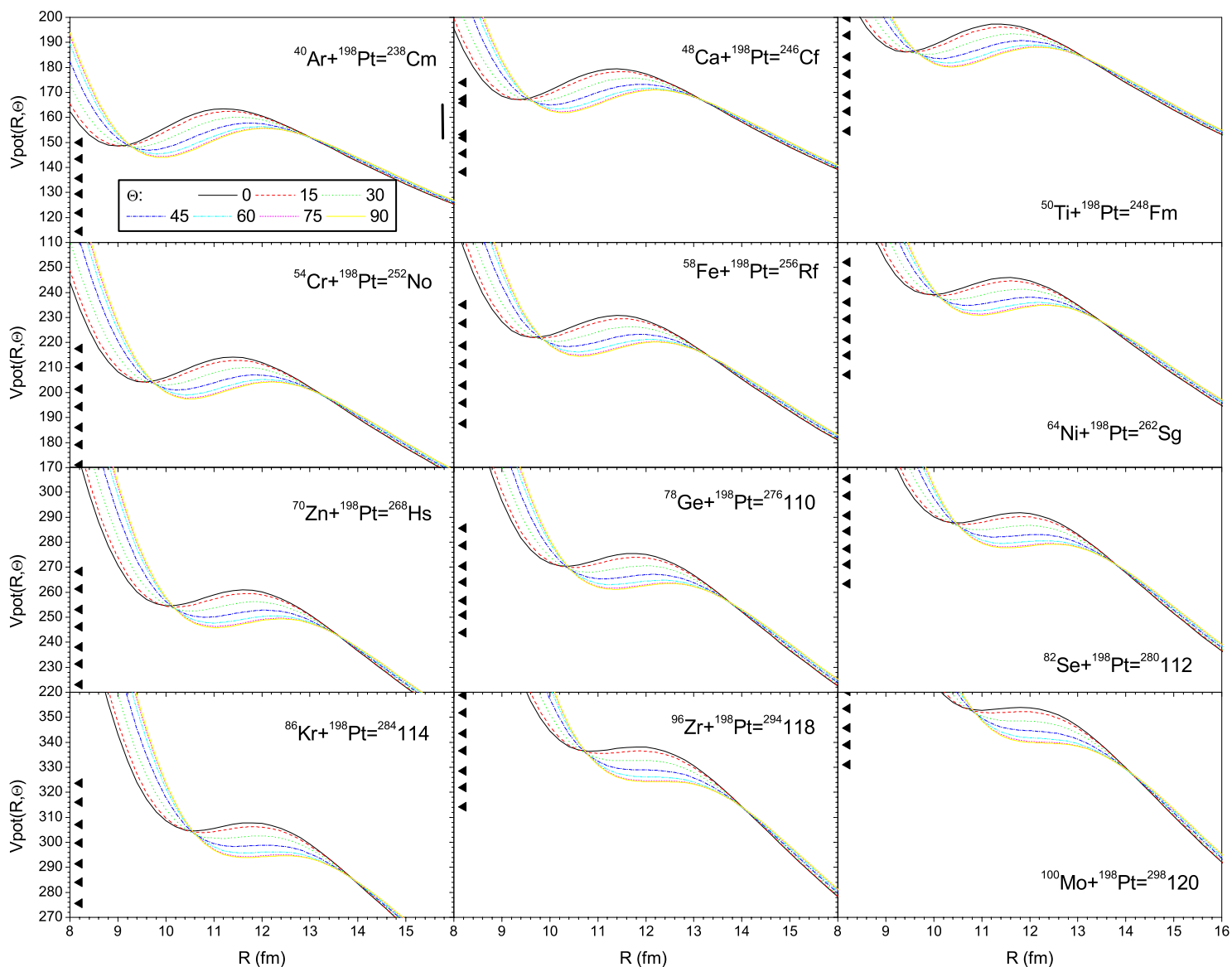
# Warm-fusion systems

$^{198}\text{Pt}$  - oblate  $-\beta_2 = -0.10$

Recent GSI experiment:  $^{40}\text{Ar}, ^{50}\text{Ti} + ^{198}\text{Pt}$ .

The cross sections for reaction  $^{50}\text{Ti} + ^{198}\text{Pt}$  is comparable with the one for cold-fusion reaction  $^{40}\text{Ar} + ^{208}\text{Pb}$ .

Large distances between spherical and oblate nuclei  $\Rightarrow \vartheta = 0^\circ$   
due to the Coulomb interaction ( $\vartheta = 0^\circ \Leftrightarrow$  'tip' position)



# Conclusion

## Rules for the determination of the best candidates for the synthesis of SHEs

- The SMP barrier should lie about 5 to 15 MeV above the 1n fusion threshold, but not above the 2n fusion threshold to avoid the reduction of the fusion cross-section by an additional factor  $\Gamma_n/\Gamma_f$
- The deeper the pocket  $\Rightarrow$  the larger the capture window  $\Rightarrow$  better the chance of synthesis
- It is best to have a most compact capture configuration

# The synthesis of 118 with **hot-**, **cold-** and **warm-**fusion systems

- The cold-fusion system  $^{86}\text{Kr}+^{208}\text{Pb}$  has its capture window below the 1n-fusion channel and shallow pocket, and hence is not expected to be a good candidate
- The symmetric system  $^{144}\text{Ce}+^{150}\text{Nd}$  has no pocket and hence no capture window at all
- The hot-fusion system  $^{48}\text{Ca}+^{252}\text{Cf}$  has nice capture properties, however needs to emit about 3 to 4 neutrons, which reduce the survival probability by several orders due to factor  $\Gamma_n/\Gamma_f \ll 1$
- The hot-fusion system  $^{40}\text{Ca}+^{252}\text{Cf}$  has less attractive capture properties (as compared to the  $^{48}\text{Ca}$  case) and needs to emit even 5 to 6 neutrons
- The system  $^{58}\text{Fe}+^{238}\text{U}$  has only a tiny pocket and needs to emit about 3-4 neutrons
- the warm-fusion system  $^{96}\text{Zr}+^{198}\text{Pt}$  has also a tiny tip-positioned pocket but needs to emit only 1n

The most attractive projectile-target are:

$$^{48}\text{Ca}+^{252}\text{Cf} \text{ at } E_{\text{coll}} \approx 206 \text{ MeV}$$

$$^{96}\text{Zr}+^{198}\text{Pt} \text{ at } E_{\text{coll}} \approx 330 \text{ MeV}.$$

While  $^{48}\text{Ca}+^{252}\text{Cf}$  is more compact,  $^{96}\text{Zr}+^{198}\text{Pt}$  needs to emit only 1 neutron.

*It is hard to judge which of these features are more important*

